ARTHRITIS & RHEUMATOLOGY
Vol. 68, No. 5, May 2016, pp 1233–1244
DOI 10.1002/art.39535

Development of Th17-Associated Interstitial Kidney Inflammation in Lupus-Prone Mice Lacking the Gene Encoding STAT-1

Gloria Yiu,[1] Tue K. Rasmussen,[2] Bahareh Ajami,[1] David J. Haddon,[1] Alvina D. Chu,[1] Stephanie Tangsombatvisit,[1] Winston A. Haynes,[1] Vivian Diep,[1] Larry Steinman,[3] James Faix,[1] and Paul J. Utz[3]

Objective. **Type I interferon (IFN) signaling is a central pathogenic pathway in systemic lupus erythematosus (SLE), and therapeutics targeting type I IFN signaling are in development. Multiple proteins with overlapping functions play a role in IFN signaling, but the signaling events downstream of receptor engagement are unclear. This study was undertaken to investigate the roles of the type I and type II IFN signaling components IFN-$\alpha/\beta/\omega$ receptor 2 (IFNAR-2), IFN regulatory factor 9 (IRF-9), and STAT-1 in a mouse model of SLE.**

Methods. **We used immunohistochemical staining and highly multiplexed assays to characterize pathologic changes in histology, autoantibody production, cytokine/chemokine profiles, and STAT phosphorylation in order to investigate the individual roles of IFNAR-2, IRF-9, and STAT-1 in MRL/*lpr* mice.**

Results. **We found that STAT-$1^{-/-}$ mice, but not IRF-$9^{-/-}$ or IFNAR-$2^{-/-}$ mice, developed interstitial nephritis characterized by infiltration with retinoic acid receptor–related orphan nuclear receptor γt–positive lymphocytes, macrophages, and eosinophils. Despite pronounced interstitial kidney disease and abnormal kidney function, STAT-$1^{-/-}$ mice had decreased proteinuria, glomerulonephritis, and autoantibody production. Phosphospecific flow cytometry revealed shunting of STAT phosphorylation from STAT-1 to STAT-3/4.**

Conclusion. **We describe unique contributions of STAT-1 to pathology in different kidney compartments in a mouse model, and provide potentially novel insight into tubulointerstitial nephritis, a poorly understood complication that predicts end-stage kidney disease in SLE patients.**

Systemic lupus erythematosus (SLE) is a chronic autoimmune disease characterized by inflammatory destruction of multiple organs. Patients are treated with glucocorticoids, nonsteroidal antiinflammatory drugs, cytotoxic agents, hydroxychloroquine, mycophenolate mofetil, and rituximab, alone or in combination (1). In the last decade, pathophysiologic pathways in SLE have been discovered and targeted. These include therapies targeting interferon-α (IFNα), a type I IFN (2).

Evidence that IFNα plays a crucial role in SLE is extensive. A subset of patients who receive IFNα for hepatitis develop an SLE-like illness, ranging from development of antinuclear antibodies to frank autoimmunity that meets the diagnostic criteria for SLE (3). Transcript profiling of bulk peripheral blood mononuclear cells and immune cell subsets from SLE patients

Supported by the NIH (grant 1-S10-OD-0105800A1 and National Heart, Lung, and Blood Institute Proteomics contract HHSN-288201000034C), the Lupus Foundation of America, the Alliance for Lupus Research (grant 21858), the Stanford Institute for Immunity, Transplantation, and Infection (pilot grant), FP grant 261, and the Henry Gustav Floren Foundation (gift to Dr. Utz). Ms Yiu's work was supported by the Stanford Medical Scientist Training Program. Dr. Rasmussen's work was supported by the Novo Nordisk Foundation, the Danish Rheumatoid Association, and The Graduate School of Health, Aarhus University. Dr. Utz is recipient of a Donald E. and Delia B. Baxter Foundation Career Development Award.

[1]Gloria Yiu, BS, Bahareh Ajami, PhD, David J. Haddon, PhD, Alvina D. Chu, MD, Stephanie Tangsombatvisit, MD, Winston A. Haynes, BS, Vivian Diep, BS, James Faix, MD: Stanford University School of Medicine, Stanford, California; [2]Tue K. Rasmussen, MD, PhD: Stanford University School of Medicine, Stanford, California, and Aarhus University, Aarhus, Denmark; [3]Larry Steinman, MD, Paul J. Utz, MD: Stanford University School of Medicine and Institute for Immunity, Transplantation, and Infection, Stanford, California.

Address correspondence to Gloria Yiu, BS, Department of Medicine, Division of Immunology and Rheumatology, Stanford University School of Medicine, CCSR Building, Room 2215A, 269 Campus Drive West, Stanford, CA 94305. E-mail: gloyiu@stanford.edu.

Submitted for publication March 17, 2015; accepted in revised form November 24, 2015.

demonstrated the presence of an IFNα-inducible gene expression signature or "IFN biosignature" (4). This biosignature has been shown to correlate with the SLE Disease Activity Index (SLEDAI) (5) and the 1997 update of the American College of Rheumatology revised criteria for SLE (6,7).

The IFN biosignature has been robustly recapitulated in murine models of SLE (8). However, results from groups studying lupus-prone mice lacking the α-chain of IFN-α/β receptor (IFN-α/βR; called IFNAR-1) are inconsistent, reporting either improved or worsened disease (9–11). Our group has defined roles for IFN-$\alpha/\beta/\omega$ receptor 2 (IFNAR-2), IFN regulatory factor 9 (IRF-9), and STAT-1 in mice with pristane-induced arthritis (12,13) (details are available from the corresponding author upon request). We identified defects in Toll-like receptor 7 (TLR-7)– and TLR-9–specific B cell responses and isotype-switched IgG autoantibodies in IFNAR-$2^{-/-}$, IRF-$9^{-/-}$, and STAT-$1^{-/-}$ mice.

Because the pristane-induced model of arthritis is an inducible model associated with mild kidney pathology, the roles of IFNAR-2, IRF-9, and STAT-1 in the spontaneous development of organ-specific involvement, such as glomerulonephritis (GN), is unclear. In the MRL/*lpr* mouse model, SLE-like pathogenesis results from a loss-of-function mutation in Fas (lymphoproliferation [*lpr*]), leading to defects in the negative selection of autoreactive B and T lymphocytes. MRL/*lpr* mice recapitulate human SLE pathologies, particularly the progressive immune complex–mediated GN seen in lupus nephritis, a leading cause of mortality (14). Other features of the model include more frequent occurrence in females, diffuse organ inflammation, and autoantibodies against DNA- and RNA-containing antigens (15).

Given the plethora of cytokines dysregulated in autoimmunity promotion (16,17), there is growing interest in shared signaling pathways, including phosphorylation of STAT family members involved in IFN signaling. Binding of IFNAR by IFNα triggers phosphorylation of STAT-1/2 by JAK family proteins. This leads to formation of a heterotrimeric complex, IFN-stimulated transcription factor 3 (ISGF-3), composed of STAT-1, STAT-2, and IRF-9. Nuclear translocation of this complex enables binding to IFN-stimulated response element (ISRE). In contrast, IFNγ binds to IFNγR and triggers phosphorylation of a STAT-1 homodimer, which binds γ-activated site–containing genes. Downstream effects of both type I and type II signaling result in gene transcription, including those vital to immune function.

In this study, we investigated the individual contributions of the type I and type II IFN signaling components IFNAR-2, IRF-9, and STAT-1 to spontaneous SLE-like pathogenesis in the MRL/*lpr* mouse model. We hypothesized that ablation of any of the 3 IFN signaling components would result in an ameliorated disease phenotype. Instead, our findings support unique roles of IFNAR-2, IRF-9, and STAT-1 and demonstrate a critical role for STAT-1 in the development of Th17 cell–associated interstitial nephritis in SLE-like disease. This pathology mimics tubulointerstitial nephritis, which correlates with end-stage renal failure in SLE patients (18). We further demonstrate marked Th17 enrichment in lymphoid organs, alterations in autoantibody profiles, and shunting of STAT-1 signaling to other cytokine pathways. Taken together, our results suggest that STAT-1 ablation leads to ameliorated glomerular disease in MRL/*lpr* mice, and to development of unanticipated effects on the immune system and interstitial nephritis.

MATERIALS AND METHODS

Mice. MRL/MpJ mice were purchased from The Jackson Laboratory. IFNAR-$2^{-/-}$ mice on the BALB/c background were kindly provided by Paul J. Hertzog (Monash University, Clayton, Victoria, Australia). IRF-$9^{-/-}$ mice on the BALB/c background were purchased from the RIKEN BioResource Center. STAT-$1^{-/-}$ mice on the BALB/c background were a generous gift from J. Durbin (Ohio State University, Columbus, OH). All knockout mice were backcrossed onto the MRL/*lpr* background (The Jackson Laboratory) to the N8–N10 generation. Data were obtained in female mice at 16 weeks of age. Every mouse analyzed in this study was genotyped for the presence or absence of the gene of interest (data available from the corresponding author upon request).

Histopathology and immunohistochemical staining. Mice were euthanized by CO_2 exposure followed by cervical dislocation. Kidneys were surgically removed, fixed in buffered formalin, embedded in paraffin, sectioned, and stained with either periodic acid–Schiff (PAS) or hematoxylin and eosin (H&E) or stained for CD45 (30-F11; BD PharMingen) (performed by Histo-Tec). The slides were scored in a blinded manner by one of the authors (JF) according to the National Institutes of Health (NIH) kidney scoring system (19) for both active and chronic disease (details are available from the corresponding author upon request).

Immunofluorescence staining. Mice were injected intraperitoneally with ketamine (100 mg/kg) and diazepam (5 mg/kg) and transcardially perfused with 30 ml of phosphate buffered saline (PBS)–EDTA followed by 30 ml of 4% paraformaldehyde (weight/volume) in 0.1*M* PBS at room temperature. Kidneys were removed and then fixed in 4% paraformaldehyde at 4°C for up to 24 hours and then cryoprotected in 24% sucrose solution (w/v) in PBS for 24 hours. Kidneys were embedded in OCT compound (Tissue-Tek), frozen at −80°C, and then cut into 7-μm sections. Sections were thawed at 20°C, rehydrated in PBS for 2 hours, and then

treated with 0.3% Triton in PBS for 30 minutes. Three hundred microliters of cold acetone was added to each section for 15 minutes at −20°C and washed with PBS 3 times. Blocking was performed with 5–10 μg/ml anti-CD16/32 for 2 hours. Primary antibody staining was performed overnight at 4°C for the following molecules: retinoic acid receptor–related orphan nuclear receptor γt (RORγt) (AFKJS-9; eBioscience), ionized calcium–binding adapter molecule 1 (IBA-1) (catalog no. 019-19741; Wako), and IgM (1020-01; SouthernBiotech). Secondary antibody staining was performed using donkey anti-goat Alexa Fluor 647, donkey anti-rabbit Alexa Fluor 568, or donkey anti-rat Alexa Fluor 488 (Molecular Probes) in the dark for 1 hour at room temperature. All sections were analyzed by confocal microscopy using either a Leica SP2 AOBS confocal microscope or a Leica SP8 confocal microscope. All images presented are maximum intensity projections of *z* stacks of individual optical sections.

Cytokine stimulation and phospho-flow cytometry. Splenocytes were cultured for at least 2 hours and stained for viability with Aqua Amine Live/Dead cell stain (Invitrogen) for 30 minutes. Following washing and resting for 30 minutes, splenocytes were stimulated with IFNα (1,000 units/ml; PBL InterferonSource), IFNγ (50 ng/ml; PeproTech), interleukin-4 (IL-4) (50 ng/ml; PeproTech), IL-12 (50 ng/ml; PeproTech,), IL-21 (50 ng/ml; PeproTech), or IL-27 (50 ng/ml; R&D Systems) for 20 minutes at 37°C. Stimulation was halted with 1.6% paraformaldehyde for 10 minutes at room temperature. Following washing with fluorescence-activated cell sorting (FACS) buffer (0.5% bovine serum albumin and 0.09% sodium azide in PBS), splenocytes were permeabilized using prechilled methanol for 20 minutes at 4°C. Following washing, cells were stained for 1 hour at room temperature with fluorophore-conjugated surface antibodies (a list is available from the corresponding author upon request). Following washing, cells were fixed with 1.6% paraformaldehyde and analyzed by LSRII (Becton Dickinson).

Additional details regarding mice, intracellular cytokine staining, lupus autoantigen microarrays, enzyme-linked immunosorbent assays (ELISAs), real-time quantitative polymerase chain reaction (qPCR), Luminex multiple cytokine/chemokine assay, and statistical methods are available from the corresponding author upon request.

RESULTS

Decreased proteinuria in mice deficient in type I or type II IFN and elevated renal function markers in STAT-1$^{-/-}$ mice. A hallmark of human and murine SLE is the development of GN, in which immune complex deposition in glomeruli results in inflammation and failure to retain proteins (20,21). We hypothesized that mice with defects in IFN signaling would have less severe inflammation and thus would be protected against GN development. We assessed proteinuria in female MRL/*lpr* mice lacking IFNAR-2 (IFNAR-2$^{-/-}$ mice), IRF-9 (IRF-9$^{-/-}$ mice), or STAT-1 (STAT-1$^{-/-}$ mice), in addition to female MRL/*lpr* and MRL/MpJ

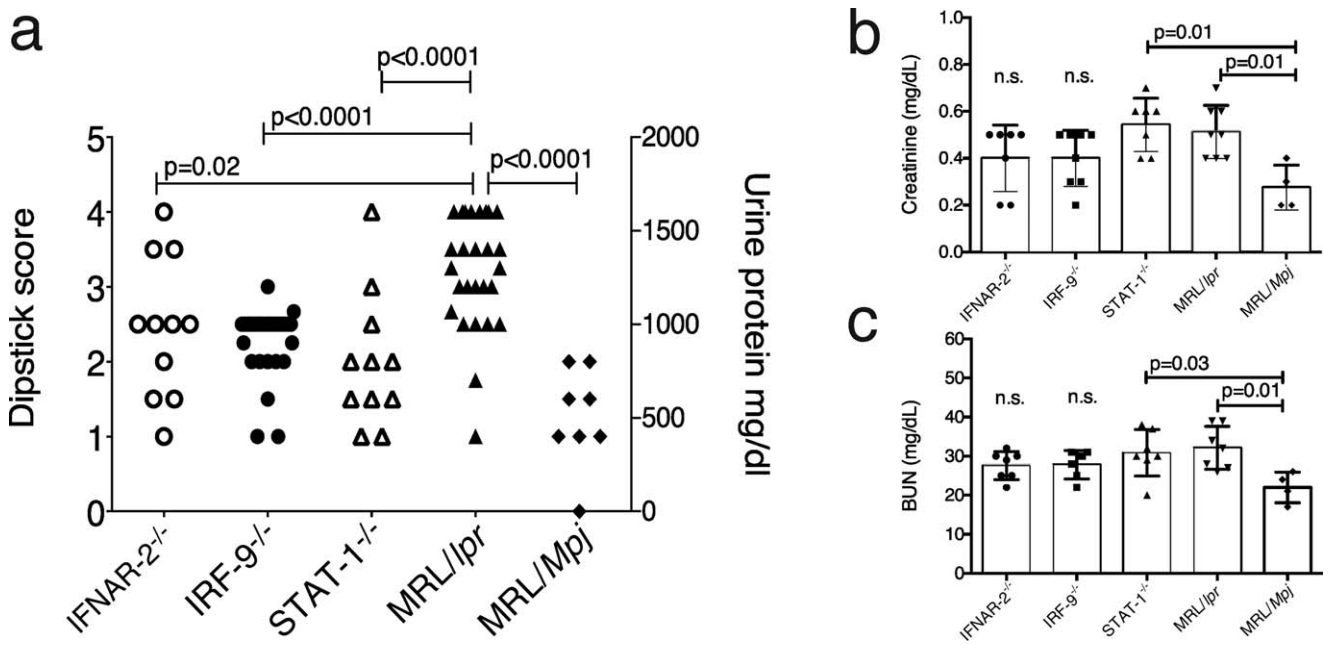

Figure 1. Decreased proteinuria and abnormal renal function in STAT-1$^{-/-}$ mice. **a,** Urinary protein levels, determined by dipstick (Bayer), in 16-week-old IFNAR-2$^{-/-}$ mice (n = 11), IRF-9$^{-/-}$ mice (n = 30), STAT-1$^{-/-}$ mice (n = 11), MRL/*lpr* mice (n = 27), and MRL/MpJ mice (n = 8). Symbols represent individual mice. **b** and **c,** Serum creatinine **(b)** and blood urea nitrogen (BUN) **(c)** levels, measured using a clinical chemistry analyzer, in IFNAR-2$^{-/-}$ mice (n = 7), IRF-9$^{-/-}$ mice (n = 8), STAT-1$^{-/-}$ mice (n = 7), MRL/*lpr* mice (n = 8), and MRL/MpJ mice (n = 4). Symbols represent individual mice; bars show the mean ± SEM. *P* values were determined by Mann-Whitney test. NS = not significant.

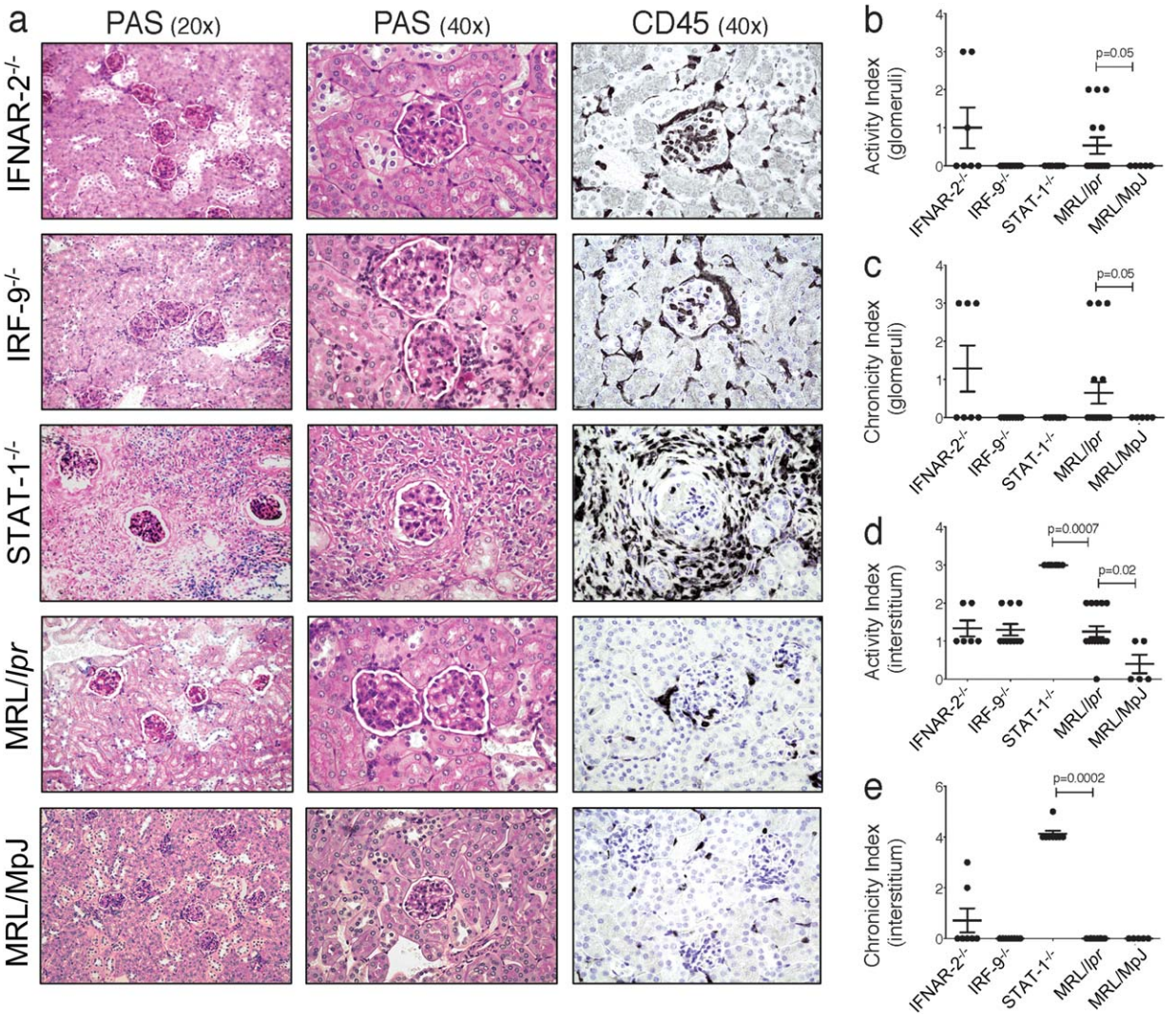

Figure 2. Increased active and chronic interstitial kidney pathology with infiltrating CD45+ immune cells in STAT-$1^{-/-}$ mice. **a,** Left, Periodic acid–Schiff (PAS) staining of 5-μm–thick sections from the indicated mouse strains. Middle, Higher-magnification views of the PAS-stained sections. Right, Staining of 5-μm–thick sections for CD45 with 3,3′-diaminobenzidine. **b–e,** Scoring of mouse kidneys using the National Institutes of Health activity and chronicity scoring system. IRF-$9^{-/-}$ and STAT-$1^{-/-}$ mice exhibited decreased active (**b**) and chronic (**c**) glomerular pathology, while IFNAR-$2^{-/-}$ mice exhibited increased active and chronic glomerular pathology. STAT-$1^{-/-}$ mice exhibited increased active (**d**) and chronic (**e**) interstitial pathology. Symbols represent individual mice; horizontal lines and error bars show the mean ± SEM (n = 7 IFNAR-$2^{-/-}$ mice, n = 10 IRF-$9^{-/-}$ mice, n = 8 STAT-$1^{-/-}$ mice, n = 11 MRL/*lpr* mice, and n = 5 MRL/MpJ mice). *P* values were determined by Mann-Whitney test.

mice, at 16 weeks to allow for disease development in organ systems including the kidneys (22). MRL/MpJ mice lack the *lpr* mutation and were used as a control strain. As expected, MRL/*lpr* mice developed significantly higher levels of proteinuria than MRL/MpJ controls ($P < 0.0001$) (Figure 1a). Mice lacking IFNAR-2, IRF-9, or STAT-1 all exhibited significantly decreased proteinuria compared to MRL/*lpr* mice ($P = 0.02$, $P < 0.0001$, and $P < 0.0001$, respectively), indicating relatively preserved glomerular function, consistent with our initial hypothesis.

IFNAR-2 and IRF-9 ablation led to decreased serum levels of both creatinine and blood urea nitrogen (BUN) compared to MRL/*lpr* mice, although the differences were not statistically significant (Figures 1b and c). As expected, MRL/*lpr* mice had significantly higher serum levels of both creatinine and BUN than MRL/MpJ mice ($P = 0.01$). Surprisingly, STAT-$1^{-/-}$ mice also exhibited increased creatinine and BUN levels compared to MRL/MpJ mice, suggesting poor renal function despite improved proteinuria ($P = 0.01$ for creatinine and $P = 0.03$ for BUN).

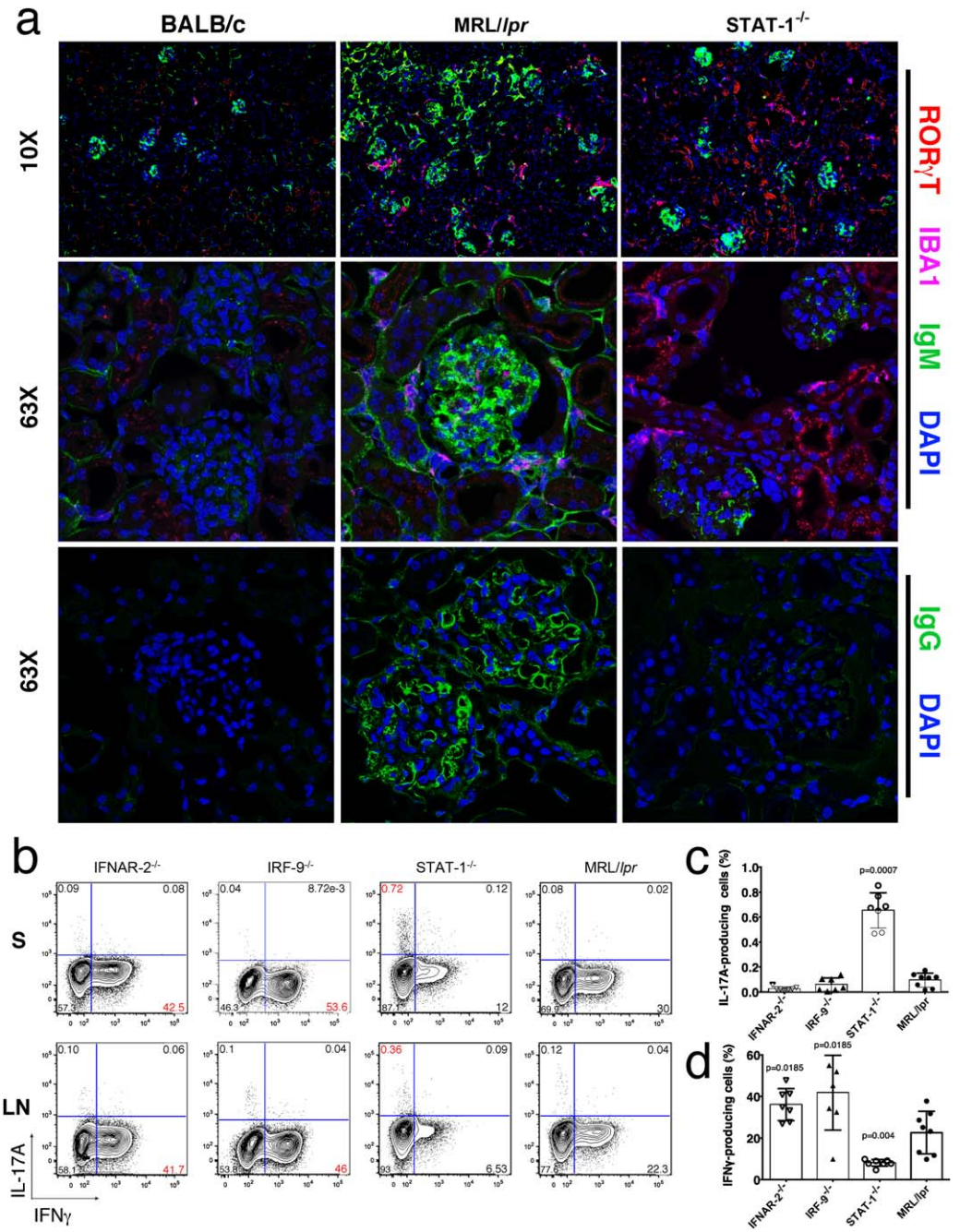

Figure 3. Differential accumulation of cells expressing retinoic acid receptor–related orphan nuclear receptor γt (RORγt) in the kidney interstitium and interleukin-17A (IL-17A)/interferon-γ (IFNγ) in secondary lymphoid organs in mice genetically deficient in IFN signaling components. **a,** Staining of 7-μm–thick frozen sections from the mouse strains indicated for RORγt (red), ionized calcium–binding adapter molecule 1 (IBA-1; magenta), IgM or IgG (green), and DAPI (blue). STAT-1$^{-/-}$ mice exhibited increased Th17 and macrophage infiltration in the interstitium. **b,** Intracellular staining of mouse spleen (S) sections (top) and lymph node (LN) sections (bottom) for IFNγ and IL-17A, showing increased frequencies of IL-17A–producing CD4+ T cells in STAT-1$^{-/-}$ mice and increased frequencies of IFNγ-producing CD4+ T cells in IRF-9$^{-/-}$ and IFNAR-2$^{-/-}$ mice. Data for BALB/c mice with and without STAT-1 deficiency are available from the corresponding author upon request. **c** and **d,** Graphical representation of flow cytometry data for IL-17A (**c**) and IFNγ (**d**) in mouse spleen cells. Symbols represent individual mice; bars show the mean ± SEM (n = 7 for IFNAR-2$^{-/-}$ mice, IRF-9$^{-/-}$ mice, and STAT-1$^{-/-}$ mice; n = 8 for MRL/*lpr* mice). *P* values are versus MRL/*lpr* mice and were determined by Mann-Whitney test.

Unexpected development of interstitial kidney disease in STAT-1$^{-/-}$ mice. Kidney disease in SLE patients can be categorized into distinctive classes in which different areas of the kidney are affected. Because proteinuria is largely a measure of glomerular damage, further experiments were performed to assess global kidney morphology. We performed PAS staining on sections prepared from paraffin-embedded mouse kidneys (Figure 2a) and quantified renal nephritis using the NIH activity and chronicity indices in a blinded manner (details are available from the corresponding author upon request).

As we predicted, IRF-9$^{-/-}$ and STAT-1$^{-/-}$ mice exhibited lower active and chronic glomerular scores than MRL/*lpr* mice, although the difference was not statistically significant (Figures 2b–e). Conversely, IFNAR-2$^{-/-}$ mouse kidneys had increased active and chronic glomerular scores as compared to MRL/*lpr* mouse kidneys, although this difference also was not statistically significant. Unexpectedly, STAT-1$^{-/-}$ mouse kidneys showed significantly increased active and chronic tubulointerstitial pathology compared to MRL/*lpr* mouse kidneys ($P = 0.0007$ and $P = 0.0002$, respectively) (Figures 2d and e). To further investigate this finding, we performed immunohistochemical staining of kidney sections for the leukocyte marker CD45 (Figure 2a). We observed marked interstitial infiltration of CD45+ leukocytes in kidneys from STAT-1$^{-/-}$ mice as compared to IFNAR-2$^{-/-}$, IRF-9$^{-/-}$, MRL/*lpr*, and MRL/MpJ mice, suggesting that an immune cell–mediated process was responsible for the tubulointerstitial disease.

Infiltration of the interstitium by RORγt-positive cells in STAT-1$^{-/-}$ mice. The GN observed in MRL/*lpr* mice is a B cell–associated process characterized by deposition of IgM/IgG (21). Elevated levels of Th17 lymphocytes, a subset of inflammatory T cells, have also been observed in both the peripheral blood and kidneys of lupus nephritis patients (23). To better characterize the immune cell infiltrate within the interstitium of knockout mice, we performed a series of immunohistochemical stainings for RORγt (the canonical transcription factor required for Th17 cell development), IBA-1 (a macrophage marker), and eosinophils. Both macrophages (24) and eosinophils (25) have been identified in the polarization and downstream function of Th17 lymphocytes.

As expected, MRL/*lpr* mouse kidneys showed increased IgM and IgG deposition in the glomeruli compared to kidneys from BALB/c mice (Figure 3a). In contrast, minimal staining for IgM and IgG was observed in the glomeruli of STAT-1$^{-/-}$ mice, suggesting that other factors and/or cell types are involved. We observed notable infiltration of RORγt-positive cells confined to the interstitium of STAT-1$^{-/-}$ mice (Figure 3a). The STAT-1$^{-/-}$ mouse interstitium also demonstrated increased H&E staining for IBA-1 (Figure 3a) and eosinophils (results are available from the corresponding author upon request). Taken together, the findings of histologic evaluation of kidney specimens indicate a role for RORγt-positive cells in mice lacking STAT-1, in contrast with the central role played by B lymphocytes in MRL/*lpr* mice with GN.

Altered Th1/Th17 polarization in mice deficient in type I and type II IFN signaling. In addition to their role in kidney disease, the circulating Th17 cell population is increased in SLE patients (26). We hypothesized that ablation of STAT-1 would lead to increased Th17 polarization in secondary lymphoid organs. We quantified the proportions of IL-17A– and IFNγ-producing lymphocytes in the mouse spleen and lymph nodes (axillary, mandibular, and mesenteric) by flow cytometry.

The proportion of IL-17A+CD4+ T cells was increased in STAT-1$^{-/-}$ mouse splenocytes by >8 fold compared to MRL/*lpr* mouse splenocytes (0.84% versus 0.10%; $P = 0.0007$) (Figures 3b and c). No significant changes were observed in the frequencies of IL-17A–producing CD4+ T cells in IFNAR-2$^{-/-}$ mice and IRF-9$^{-/-}$ mice (0.15% and 0.04%, respectively) as compared to MRL/*lpr* mice (Figures 3b and c). To test whether the absence of STAT-1 alone would lead to expansion of the Th17 lymphocyte population, intracellular cytokine staining of IL-17A was also performed on BALB/c mouse splenocytes lacking STAT-1. No significant enrichment was found when compared to wild-type BALB/c mice (data are available from the corresponding author upon request).

As expected, fewer IFNγ-producing CD4+ T cells were observed in the spleen and lymph nodes obtained from STAT-1$^{-/-}$ mice than in cells obtained from MRL/*lpr* mice (12.12% and 30.02%, respectively, in the spleen; $P = 0.004$) (Figures 3b and d). IFNAR-2$^{-/-}$ and IRF-9$^{-/-}$ mice had significantly larger populations of IFNγ-producing CD4+ T cells in the spleen (42.56% and 53.6%, respectively; $P = 0.0185$) (Figures 3b and d). These results suggest cross-talk between type I IFN and type II IFN signaling. In the absence of type I IFN signaling proteins, a compensatory increase in IFNγ signaling is observed, likely mediated by STAT-1 shunting.

Decreased production of IgM/IgG autoantibodies against SLE-associated antigens in STAT-1$^{-/-}$ mice. Antibodies directed against autoantigens are clinically relevant in GN (27), while the role of autoantibodies in interstitial kidney disease is not well understood.

We used protein microarrays to profile autoantibodies in the sera of our mice. This method has been well established by our laboratory for studying human SLE (28–30) and murine SLE (12,13,31). Briefly, arrays containing >600 features and 100 unique proteins and peptides were printed and probed with sera, and bound autoantibodies were detected with a fluorophore-conjugated secondary antibody. Arrays were scanned, and fluorescence intensity was quantitated. The Significance Analysis of Microarrays (SAM) algorithm (32) was used to determine antigens with statistically significant differences between groups of mice, and a hierarchical clustering program was used to group individual mice based on similar autoantibody profiles.

IgM autoantibody reactivity against SLE-associated autoantigens was decreased in STAT-$1^{-/-}$ mice compared to MRL/*lpr* mice (Figure 4a). SAM identified 12 of these IgM autoantibodies as significantly decreased in STAT-$1^{-/-}$ mouse sera compared to MRL/*lpr* mouse sera. Differentially targeted autoantigens included U1 small nuclear RNP, histones, and double-stranded DNA, all of which are important in human SLE. SAM identified a similar but constricted subset of IgG autoantibodies that were significantly decreased in STAT-$1^{-/-}$ compared to MRL/*lpr* mouse sera (Figure 4b).

When comparing IRF-$9^{-/-}$ and MRL/*lpr* mouse sera, SAM identified increased IgM and IgG autoantibody reactivity against histones in IRF-$9^{-/-}$ mouse sera (results are available from the corresponding author upon request). These data reveal a potentially unique role for IRF-9 in antibody production against histones. We did not identify any antigens with significantly different reactivity when comparing IFNAR-$2^{-/-}$ and MRL/*lpr* mouse sera. Of 22 significant array findings, 17 were validated as significant using ELISA (Figure 4c) (data are available from the corresponding author upon request).

STAT-1 is required for the expression and up-regulation of TLR-7 by IFNα. Nucleic acid components of SLE autoantigens can activate autoreactive B cells via TLRs. TLR expression is also up-regulated by type I IFN secreted by plasmacytoid dendritic cells in human naive B cells and modulates isotype switching (33). We have previously demonstrated in the pristane-induced model that mice lacking IFNAR-2, IRF-9, or STAT-1 have defects in up-regulating TLR-7 and/or TLR-9 expression in response to IFNα exposure (12,13). Moreover, STAT-$1^{-/-}$ mice with pristane-induced arthritis had a marked defect in isotype switching of autoantigen-specific B cells, but not B cells immunized with ovalbumin. We hypothesized that the decreased autoantibody production observed in STAT-$1^{-/-}$ MRL/*lpr* mice was due to a similar defect in TLR-7/9 up-regulation.

Splenic B cells were obtained from STAT-$1^{-/-}$ and MRL/*lpr* mice and cultured in the presence or absence of IFNα, and relative expression levels of mRNA for TLR-7, TLR-9, and Mx1 (a known IFNα-inducible gene) were determined by real-time qPCR. The expression of TLR-7, but not TLR-9, was significantly up-regulated in IFNα-treated B cells from MRL/*lpr* mice, but this up-regulation was abolished in STAT-$1^{-/-}$ mouse B cells (Figure 4d). We conclude that STAT-1 is required for IFNα-inducible expression of TLR-7, but not TLR-9, in murine B cells. Because STAT-$1^{-/-}$ mice have decreased reactivity against both DNA- and RNA-associated antigens, these data suggest overlap of RNA/DNA-sensing by TLR-7/TLR-9 (34). Alternatively, it is possible that defects in autoantibody production in STAT-$1^{-/-}$ mice result from TLR-independent pathways.

As expected, induction of expression of Mx-1 mRNA was significantly decreased in B cells from STAT-$1^{-/-}$ mice compared to MRL/*lpr* mouse B cells ($P = 0.016$) (Figure 4e). Notably, however, STAT-$1^{-/-}$ mouse B cells stimulated with IFNα retained the ability to significantly up-regulate Mx-1 expression as compared to unstimulated cells ($P = 0.02$) (Figure 4e), revealing that STAT-1 is dispensable for IFNα signaling. This finding supports work demonstrating high redundancy and plasticity of STAT phosphorylation in different physiologic states (35,36). We tested the hypothesis that IFNα signaling can signal through molecules other than STAT-1 using phospho-flow cytometry.

Shunting of STAT phosphorylation to different cytokine signaling pathways after disruption of genes encoding type I and type II IFN signaling proteins. Several groups have demonstrated that dysregulated STAT signaling plays a role in murine models of SLE and in human SLE patients (37). We hypothesized that both Th1/Th17 polarization and transcription events downstream of IFNα signaling that are observed in the absence of type I and type II IFN signaling proteins could be attributed to dysregulated STAT signaling.

Splenocytes from individual mice were isolated and stimulated with individual cytokines for 20 minutes. We then used phospho-flow cytometry to measure the phosphorylation of STATs 1, 3, 4, 5, and 6 in CD4+ T cells (CD3+CD4+CD8−), CD8+ T cells (CD3+CD4−CD8+), and B cells (CD3−CD4−CD19+) from our mice. We selected cytokines thought to play critical roles in SLE pathogenesis, including IFNα, IFNγ, IL-21, and IL-27 (4,17). To identify additional cytokines to include in

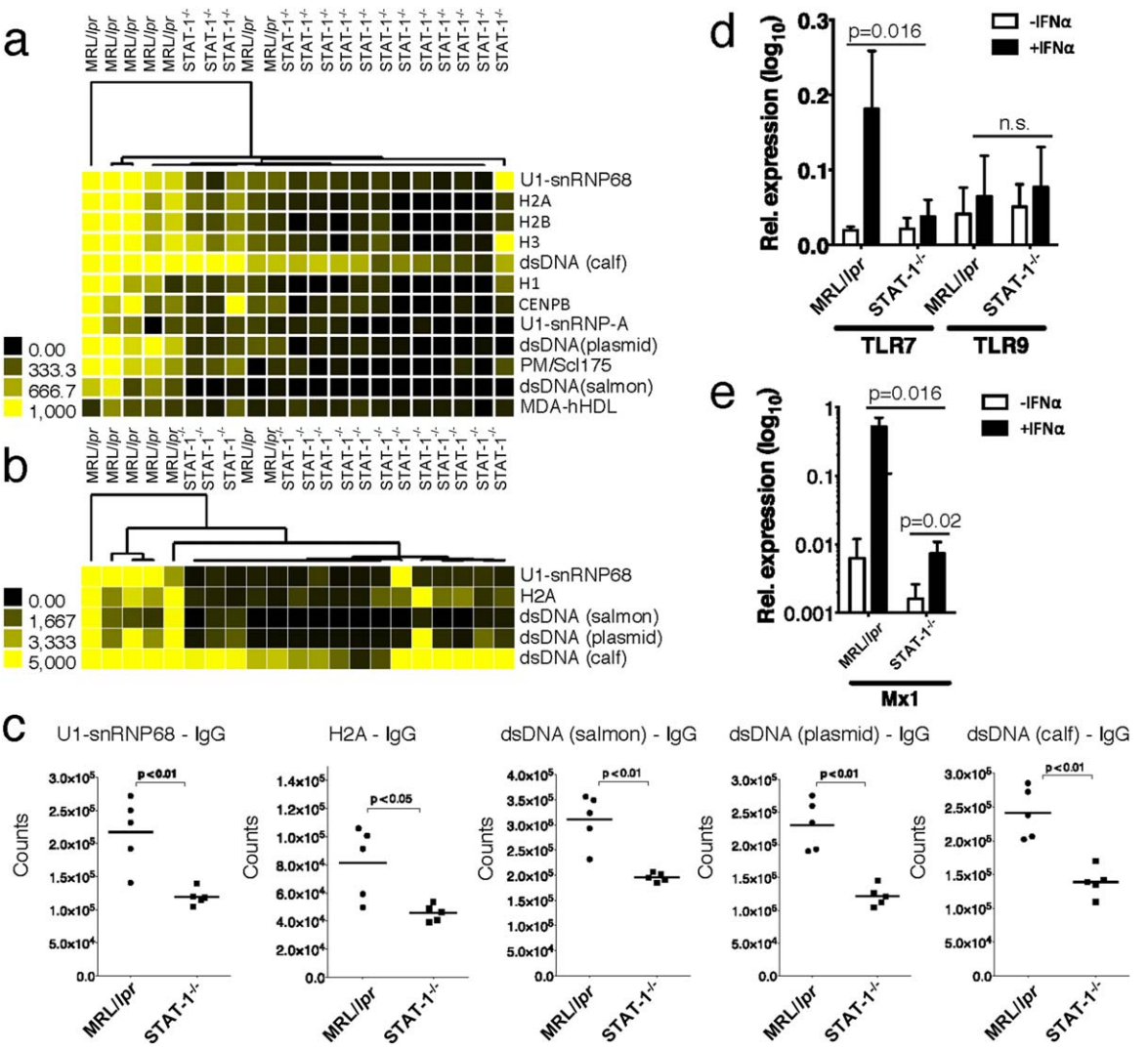

Figure 4. Reduced levels of autoantibodies against systemic lupus erythematosus–associated antigens in STAT-1$^{-/-}$ mice. Individual autoantigen arrays containing >600 features and 100 antigens were incubated with serum from MRL/*lpr*, IFNAR-2$^{-/-}$, STAT-1$^{-/-}$, or IRF-9$^{-/-}$ mice. The Significance Analysis of Microarrays (SAM) algorithm was used to determine antigen features with statistically significant differences in reactivity between sera from MRL/*lpr*, STAT-1$^{-/-}$, IRF-9$^{-/-}$, and IFNAR-2$^{-/-}$ mice. **a** and **b,** Hierarchical clustering of samples based on antigen reactivity with statistically significant differences, displayed as a heatmap and dendrogram. Sera from STAT-1$^{-/-}$ and MRL/*lpr* mice were used to probe autoantigen arrays and detected with anti-IgM (**a**) and anti-IgG (**b**) secondary antibodies. Sera from IRF-9$^{-/-}$ and MRL/*lpr* mice were subjected to the same methods (data available from the corresponding author upon request). **c,** Confirmation of SAM-identified IgG autoantibodies by enzyme-linked immunosorbent assay. (Data for IgM autoantibodies are available from the corresponding author upon request.) Data are the time-resolved fluorescence. Symbols represent individual mice; horizontal lines show the mean count (n = 5 mice per group). *P* values were determined by Mann-Whitney test. **d** and **e,** Relative expression of Toll-like receptor 7 (TLR-7) and TLR-9 (**d**) and of Mx-1 (**e**) in STAT-1$^{-/-}$ and MRL/*lpr* mouse B cells stimulated alone or with interferon-α (IFNα) for 4 hours. *P* values were determined by Mann-Whitney test. U1 sRNP68 = U1 small nuclear RNP 68; dsDNA = double-stranded DNA.

the stimulation panel, we performed a multiplex bead-based assay on STAT-1$^{-/-}$, IFNAR-2$^{-/-}$, IRF-9$^{-/-}$, and MRL/*lpr* mouse serum to determine levels of 26 different cytokines and chemokines (results are available from the corresponding author upon request). Compared to MRL/*lpr* mouse sera, sera from STAT-1$^{-/-}$ mice had significantly increased levels of TNFα, IL-4, and eotaxin 1, in addition to significantly decreased levels of IL-12p40, a cytokine that is critical for Th1 polarization (38). IRF-9$^{-/-}$ mouse sera also had significantly increased levels of IL-4 and IL-1a compared to MRL/*lpr* mouse sera. Based on these findings, IL-4 and IL-12 were added to our stimulation panel.

Phospho-flow profiling resulted in 1,980 data nodes, where each node represents phosphorylation lev-

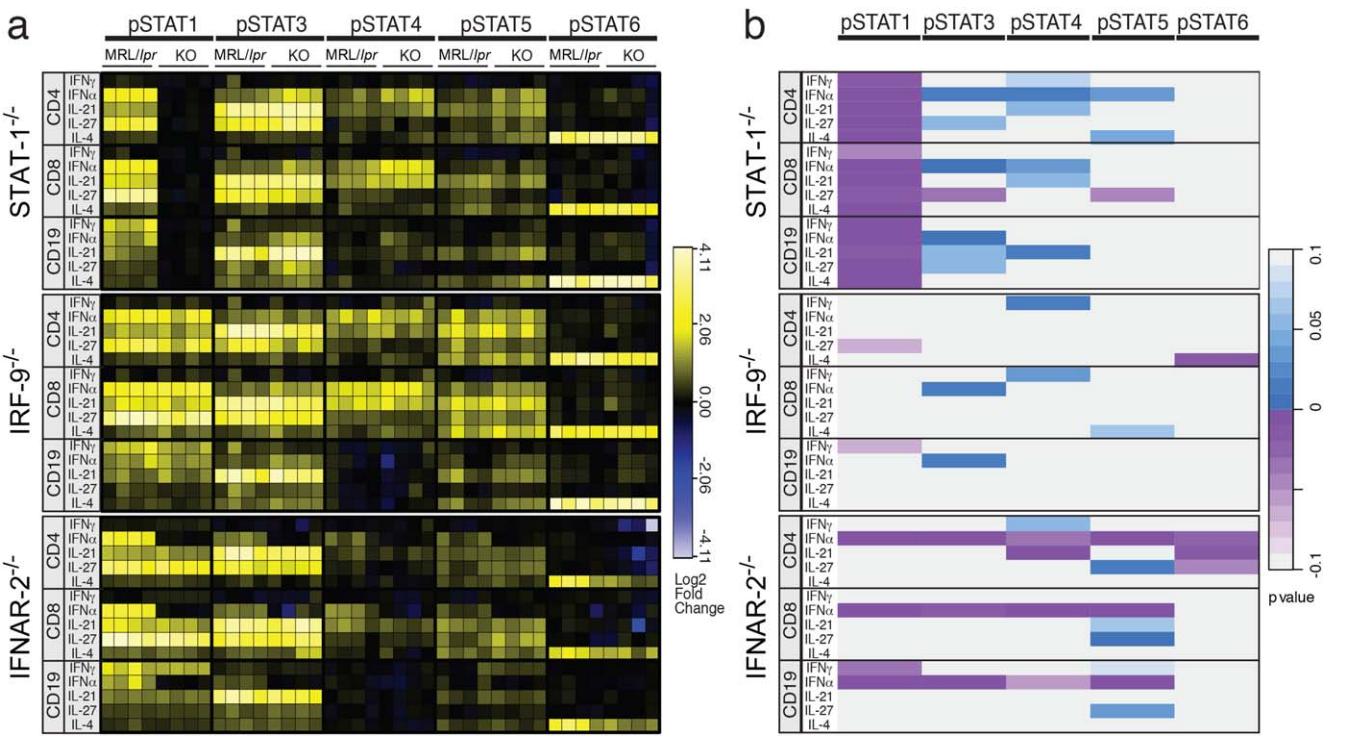

Figure 5. Shunting of STAT phosphorylation downstream of cytokine stimulation upon targeted deletion of genes encoding types I and II interferon (IFN) signaling proteins. Splenocytes from STAT-$1^{-/-}$, IRF-$9^{-/-}$, IFNAR-$2^{-/-}$, and MRL/*lpr* mice were stimulated with IFNγ, IFNα, interleukin-21 (IL-21), IL-27, or IL-4. Phosphorylation of STATs 1, 3, 4, 5, and 6 in CD4+ T cells, CD8+ T cells, and CD19+ B cells was measured by phosphospecific flow cytometry. **a,** Fold change of cytokine levels in stimulated versus unstimulated cells from individual knockout (KO) or MRL/*lpr* mice, shown in heatmap form (data were $\log_2$ transformed). Yellow and blue represent increases and decreases, respectively, in phosphorylation levels compared to baseline. Four representative mice were selected per group. **b,** Phosphorylation of individual STAT proteins downstream of an individual cytokine in one cell subset compared to corresponding data in MRL/*lpr* mice. Uncorrected *P* values, determined by Mann-Whitney test, are represented in heatmap format. Increases and decreases in STAT phosphorylation in STAT-$1^{-/-}$ mice (n = 6), IRF-$9^{-/-}$ mice (n = 4), and IFNAR-$2^{-/-}$ mice (n = 6) in comparison to MRL/*lpr* mice (n = 6) are represented by blue and purple, respectively. Bar charts of data indicating significance of fold change are available from the corresponding author upon request.

els of an individual STAT protein, in response to a single stimulation in a unique cell subset. STAT-$1^{-/-}$ mice showed no STAT-1 phosphorylation across all cell subsets (Figure 5a). In response to IFNα, STAT-3 phosphorylation was significantly increased in all subsets of STAT-$1^{-/-}$ mice compared to MRL/*lpr* mice (results are available from the corresponding author upon request). IFNα stimulation also resulted in significantly increased STAT-4 phosphorylation, in both CD4+ and CD8+ T cells from STAT-$1^{-/-}$ mice compared to MRL/*lpr* mice. These data strongly suggest that IFNα can signal through STAT-3/4.

IRF-$9^{-/-}$ mice had increased STAT-3 phosphorylation in CD8+ T cells as well as in CD19+ B cells after IFNα stimulation. Significantly increased STAT-4 phosphorylation was observed in CD4+ and CD8+ T cells from IRF-$9^{-/-}$ mice in response to IFNγ stimulation compared to MRL/*lpr* T cells (results are available from the corresponding author upon request). All cell subsets in IFNAR-$2^{-/-}$ mice exhibited significantly reduced phosphorylation of STATs 1, 3, 4, and 5 in response to IFNα stimulation compared to MRL/*lpr* mice (results are available from the corresponding author upon request). Interestingly, enhanced phosphorylation of STAT-5 in response to IL-27 was significantly observed in both CD4+ and CD8+ T cells from IFNAR-$2^{-/-}$ mice compared to MRL/*lpr* mice. This result shows that in the absence of IFNAR-2, IL-27 signaling can be modulated from phosphorylation of STAT-1/3 to phosphorylation of STAT-5. It serves as additional evidence of STAT redundancy in different biologic states.

DISCUSSION

Using highly multiplexed analyses, we showed how loss of the individual type I and type II IFN signaling molecules IFNAR-2, IRF-9, and STAT-1 affects renal disease, autoantibody profiles, T cell subsets, and

cytokine signal transduction. Notably, genetic deletion of STAT-1 leads to decreased autoantibody production and GN, but induces severe interstitial inflammation accompanied by infiltration of RORγt+ cells, CD45+ leukocytes, macrophages, and eosinophils in the interstitium. STAT-1 ablation results in altered signal transduction characterized by shunting to STAT molecules, including STAT-3, a key transcription factor involved in Th17 cell differentiation. Our findings demonstrate a critical role for STAT-1 in the development of Th17-associated autoimmune interstitial kidney disease in a murine model of SLE.

Prevention and treatment of kidney disease is a crucial aspect of the management of SLE. Despite a reported prevalence of tubulointerstitial nephritis in SLE kidney biopsy specimens ranging from 23% to 72% (18,39), little is known regarding the immunologic mechanisms underlying tubulointerstitial nephritis. Most histologic measures focus on glomerular involvement to inform therapeutic decisions, but have suboptimal predictive value in renal outcomes. In contrast, multiple groups have shown that SLE patients with tubulointerstitial nephritis are at greatest risk of renal failure, requiring long-term dialysis or renal transplantation (18,40). Our results support this model, since only STAT-$1^{-/-}$ mice with predominant tubulointerstitial nephritis, and not IFNAR-$2^{-/-}$, IRF-$9^{-/-}$, or MRL/*lpr* mice with predominant GN, showed elevation in the kidney markers BUN and creatinine. These results suggest that tubulointerstitial nephritis, more so than GN, contributes to decreased renal function in MRL/*lpr* mice.

IL-17A is thought to play an important role in SLE pathogenesis (41). The proportion of Th17 cells in the blood of SLE patients is elevated and correlates with the SLEDAI and with the presence of lupus nephritis (23). IL-17 levels are also elevated in SLE sera (42). Kidney-specific expression of IL-17A–producing cells is more controversial (43,44). We instead focused on the transcription factor RORγt. We demonstrated RORγt staining in the renal interstitium with concurrent staining of IBA-1 in STAT-$1^{-/-}$ mice but not in MRL/*lpr* mice. Costaining of eosinophils with RORγt+ cells in the interstitium of STAT-$1^{-/-}$ mice as compared to MRL/*lpr* mice further supports Th17 lymphocyte activity, since IL-17A up-regulates various cytokines that promote eosinophilic inflammation (25). Multiplexed cytokine profiling studies also revealed increased levels of serum eotaxin 1, an eosinophil chemotactic chemokine, in STAT-$1^{-/-}$ mice compared to MRL/*lpr* mice. FACS analysis demonstrated significantly higher proportions of Th17 cells in lymph nodes and splenocytes derived from STAT-$1^{-/-}$ mice compared to MRL/*lpr* mice. These data robustly support a role for STAT-1 in inhibiting Th17 lymphocyte polarization and trafficking to kidney interstitium in MRL/*lpr* mice.

Despite our findings, our study is limited by the inability to dissect independent effects of STAT-1 ablation on immune and renal parenchyma cells. Previous work has described elevated levels of IFNγ mRNA in MRL/*lpr* mouse renal cells themselves (45), resulting in the increased production of inflammatory cytokines, which induce apoptosis of cells involved in interstitial homeostasis (46). Our finding of severe Th17-associated tubulointerstitial disease is unexpected in the setting of STAT-1 ablation, since IFNγ signaling requires STAT-1 translocation to the nucleus. Adoptive transfer of STAT-$1^{-/-}$ mouse hematopoietic stem cells or IL-17–producing cells into MRL/*lpr* mice was unsuccessful due to difficulty with breeding and radiosensitivity of the MRL/*lpr* background strain. Further experiments are planned to shed light on the independent role of STAT-1 in renal versus hematopoietic cells.

Analysis of cytokine production and STAT phosphorylation in STAT-$1^{-/-}$ mouse splenocytes allowed us to investigate signaling mechanisms that could help explain differences observed in T helper cell polarization. We hypothesized that Th17 cell enrichment was associated with compensatory STAT-3/4 phosphorylation, both previously described in Th17 cell polarization (47). Our phospho-flow profiling data support this hypothesis, as STAT-$1^{-/-}$ mouse splenocytes exhibited shunted phosphorylation to STAT-3/4 downstream of multiple stimuli, including IFNα, IL-21, and IL-27, and across multiple cell subsets. Phosphorylation of other STAT proteins in response to IFNα supports our qPCR data showing that STAT-$1^{-/-}$ mouse B cells retain the capacity to up-regulate the transcription of the IFN-inducible gene Mx-1 upon IFNα receptor ligation, presumably mediated by STAT-3/4.

Phospho-flow data show no IFNα signaling in IFNAR-$2^{-/-}$ mice; however, these mice still have prominent autoantibody production and have marginally increased kidney pathology. Both of these indices have been associated with high IFN signaling rather than absence of IFN signaling (7,8). One potential explanation for the discrepancy between phenotypes of IFNAR-$2^{-/-}$ and STAT-$1^{-/-}$ mice is that MRL/*lpr* pathology is driven by IFNγ, which requires STAT-1 for signal transduction through its receptor, and that IFNα is less influential. However, evidence shows that both IFNα and IFNγ induce the formation of the ISGF-3 complex and bind to ISRE and γ-activated site, respectively (48). IFNα- and IFNγ-inducible genes have

~25% overlap, and the genes most highly up-regulated by IFNα are also IFNγ inducible (49). Notably, it remains unclear how IFN binding to receptors may be altered in the absence of a receptor subunit like IFNAR-2 (50).

Treatment of MRL/*lpr* mice with a monoclonal anti-IFNAR antibody ameliorates disease at early time points. At later stages of disease, type I IFN signaling–independent pathways overcome the therapeutic effects (51). Mangini et al (52) posit that one of these pathways is downstream of IFNγ, suggesting interactions between type I and type II IFN signaling pathways. We demonstrate direct evidence of cross-talk with increased IFNγ production in the secondary lymphoid organs of IFNAR-2$^{-/-}$ and IRF-9$^{-/-}$ mice. Cross-talk can likely be attributed to shared phosphorylation of STAT-1 downstream of IFNα and IFNγ and promiscuity of STAT phosphorylation.

Our studies highlight the complexity of type I and type II IFN signaling and the necessity for mechanistic studies in implementing therapies targeting IFNs and JAK/STATs. Our STAT-1$^{-/-}$ mouse model of Th17-associated tubulointerstitial nephritis may lead to a better understanding of JAK/STAT inhibitors like tofacitinib, which inhibits JAK-1/3. While there are no reports of tofacitinib-induced tubulointerstitial nephritis, no murine studies have addressed the effects of JAK-1/3 inhibition on autoimmune nephropathy. The IFN-targeted therapies sifalimumab (MEDI-545) and rontalizumab (RG7415) are still in early-stage clinical trials, and may be beneficial in specific subsets of patients (2). Taken together, the findings of the present study reveal unique contributions of IFN signaling proteins to SLE pathogenesis and highlight a role for STAT-1 in interstitial kidney disease in MRL/*lpr* mice. These results improve our understanding of clinically important tubulointerstitial nephritis and will guide studies of targeted therapies in patients.

ACKNOWLEDGMENTS

The authors thank Paul J. Hertzog (Monash University, Clayton, Victoria, Australia) for IFNAR-2$^{-/-}$ mice on the BALB/c background, J. Durbin (Ohio State University, Columbus, OH) for STAT-1$^{-/-}$ mice on the BALB/c background, and other members of the Utz and Steinman laboratory for technical assistance and meaningful discussions.

AUTHOR CONTRIBUTIONS

All authors were involved in drafting the article or revising it critically for important intellectual content, and all authors approved the final version to be published. Dr. Utz had full access to all of the data in the study and takes responsibility for the integrity of the data and the accuracy of the data analysis.

Study conception and design. Yiu, Rasmussen, Ajami, Haddon, Chu, Steinman, Faix, Utz.
Acquisition of data. Yiu, Rasmussen, Ajami, Haddon, Tangsombatvisit, Diep, Utz.
Analysis and interpretation of data. Yiu, Rasmussen, Ajami, Haddon, Haynes, Utz.

REFERENCES

1. Xiong W, Lahita RG. Pragmatic approaches to therapy for systemic lupus erythematosus. Nat Rev Rheumatol 2014;10:97–107.
2. Petri M, Wallace DJ, Spindler A, Chindalore V, Kalunian K, Mysler E, et al. Sifalimumab, a human anti–interferon-α monoclonal antibody, in systemic lupus erythematosus: a phase I randomized, controlled, dose-escalation study. Arthritis Rheum 2013;65:1011–21.
3. Ronnblom LE, Alm GV, Oberg K. Autoimmune phenomena in patients with malignant carcinoid tumors during interferon-α treatment. Acta Oncol 1991;30:537–40.
4. Baechler EC, Batliwalla FM, Karypis G, Gaffney PM, Ortmann WA, Espe KJ, et al. Interferon-inducible gene expression signature in peripheral blood cells of patients with severe lupus. Proc Natl Acad Sci U S A 2003;100:2610–5.
5. Bombardier C, Gladman DD, Urowitz MB, Caron D, Chang DH, and the Committee on Prognosis Studies in SLE. Derivation of the SLEDAI: a disease activity index for lupus patients. Arthritis Rheum 1992;35:630–40.
6. Hochberg MC, for the Diagnostic and Therapeutic Criteria Committee of the American College of Rheumatology. Updating the American College of Rheumatology revised criteria for the classification of systemic lupus erythematosus [letter]. Arthritis Rheum 1997;40:1725.
7. Bauer JW, Baechler EC, Michelle Petri, Batliwalla FM, Crawford D, Ortmann WA, et al. Elevated serum levels of interferon-regulated chemokines are biomarkers for active human systemic lupus erythematosus. PLoS Med 2006;3:e491.
8. Lu Q, Shen N, Li XM, Chen SL. Genomic view of IFN-α response in pre-autoimmune NZB/W and MRL/lpr mice. Genes Immun 2007;8:590–603.
9. Santiago-Raber ML, Baccala R, Haraldsson KM, Choubey D, Stewart TA, Kono DH, et al. Type-I interferon receptor deficiency reduces lupus-like disease in NZB mice. J Exp Med 2003; 197:777–88.
10. Braun D, Geraldes P, Demengeot J. Type I Interferon controls the onset and severity of autoimmune manifestations in lpr mice. J Autoimmun 2003;20:15–25.
11. Hron JD, Peng SL. Type I IFN protects against murine lupus. J Immunol 2004;173:2134–42.
12. Thibault DL, Chu AD, Graham KL, Balboni I, Lee LY, Kohlmoos C, et al. IRF9 and STAT1 are required for IgG autoantibody production and B cell expression of TLR7 in mice. J Clin Invest 2008;118:1417–26.
13. Thibault DL, Graham KL, Lee LY, Balboni I, Hertzog PJ, Utz PJ. Type I interferon receptor controls B-cell expression of nucleic acid-sensing Toll-like receptors and autoantibody production in a murine model of lupus. Arthritis Res Ther 2009;11:R112.
14. Ward MM, Pyun E, Studenski S. Causes of death in systemic lupus erythematosus: long-term followup of an inception cohort. Arthritis Rheum 1995;38:1492–9.
15. Theofilopoulos AN, Dixon FJ. Murine models of systemic lupus erythematosus. Adv Immunol 1985;37:269–390.
16. Ishida H, Muchamuel T, Sakaguchi S, Andrade S, Menon S, Howard M. Continuous administration of anti-interleukin 10 antibodies delays onset of autoimmunity in NZB/W F1 mice. J Exp Med 1994;179:305–10.
17. Viallard JF, Pellegrin JL, Ranchin V, Schaeverbeke T, Dehais J, Longy-Boursier M, et al. Th1 (IL-2, interferon-gamma (IFN-γ)) and Th2 (IL-10, IL-4) cytokine production by peripheral blood

mononuclear cells (PBMC) from patients with systemic lupus erythematosus (SLE). Clin Exp Immunol 1999;115:189–95.
18. Hsieh C, Chang A, Brandt D, Guttikonda R, Utset TO, Clark MR. Predicting outcomes of lupus nephritis with tubulointerstitial inflammation and scarring. Arthritis Care Res (Hoboken) 2011;63:865–74.
19. Austin HA 3rd, Muenz LR, Joyce KM, Antonovych TT, Balow JE. Diffuse proliferative lupus nephritis: identification of specific pathologic features affecting renal outcome. Kidney International 1984;25:689–95.
20. Winfield JB, Faiferman I, Koffler D. Avidity of anti-DNA antibodies in serum and IgG glomerular eluates from patients with systemic lupus erythematosus: association of high avidity antinative DNA antibody with glomerulonephritis. J Clin Invest 1977;59:90–6.
21. Pankewycz OG, Migliorini P, Madaio MP. Polyreactive autoantibodies are nephritogenic in murine lupus nephritis. J Immunol 1987;139:3287–94.
22. Hou LF, He SJ, Li X, Yang Y, He PL, Zhou Y, et al. Oral administration of artemisinin analog SM934 ameliorates lupus syndromes in MRL/lpr mice by inhibiting Th1 and Th17 cell responses. Arthritis Rheum 2011;63:2445–55.
23. Chen DY, Chen YM, Wen MC, Hsieh TY, Hung WT, Lan JL. The potential role of Th17 cells and Th17-related cytokines in the pathogenesis of lupus nephritis. Lupus 2012;21:1385–96.
24. Wong CK, Lit LC, Tam LS, Li EK, Wong PT, Lam CW. Hyperproduction of IL-23 and IL-17 in patients with systemic lupus erythematosus: implications for Th17-mediated inflammation in auto-immunity. Clin Immunol 2008;127:385–93.
25. Dias PM, Banerjee G. The role of Th17/IL-17 on eosinophilic inflammation. J Autoimmun 2013;40:9–20.
26. Yang J, Chu Y, Yang X, Gao D, Zhu L, Yang X, et al. Th17 and natural Treg cell population dynamics in systemic lupus erythematosus. Arthritis Rheum 2009;60:1472–83.
27. Kurts C, Panzer U, Anders HJ, Rees AJ. The immune system and kidney disease: basic concepts and clinical implications. Nat Rev Immunol 2013;13:738–53.
28. Liu CL, Tangsombatvisit S, Rosenberg JM, Mandelbaum G, Gillespie EC, Gozani OP, et al. Specific post-translational histone modifications of neutrophil extracellular traps as immunogens and potential targets of lupus autoantibodies. Arthritis Res Ther 2012;14:R25.
29. Robinson WH, DiGennaro C, Hueber W, Haab BB, Kamachi M, Dean EJ, et al. Autoantigen microarrays for multiplex characterization of autoantibody responses. Nat Med 2002;8:295–301.
30. Price JV, Tangsombatvisit S, Xu G, Yu J, Levy D, Baechler EC, et al. On silico peptide microarrays for high-resolution mapping of antibody epitopes and diverse protein-protein interactions. Nat Med 2012;18:1434–40.
31. Sekine H, Graham KL, Zhao S, Elliott MK, Ruiz P, Utz PJ, et al. Role of MHC-linked genes in autoantigen selection and renal disease in a murine model of systemic lupus erythematosus. J Immunol 2006;177:7423–34.
32. Tusher VG, Tibshirani R, Chu G. Significance analysis of microarrays applied to the ionizing radiation response. Proc Natl Acad Sci U S A 2001;98:5116–21.
33. Cerutti A, Qiao X, He B. Plasmacytoid dendritic cells and the regulation of immunoglobulin heavy chain class switching. Immunol Cell Biol 2005;83:554–62.
34. Lee BL, Moon JE, Shu JH, Yuan L, Newman ZR, Schekman R, et al. UNC93B1 mediates differential trafficking of endosomal TLRs. Elife 2013;2:e00291.
35. Papin JA, Palsson BO. The JAK-STAT signaling network in the human B-cell: an extreme signaling pathway analysis. Biophys J 2004;87:37–46.
36. Lin JX, Migone TS, Tseng M, Friedmann M, Weatherbee JA, Zhou L, et al. The role of shared receptor motifs and common stat proteins in the generation of cytokine pleiotropy and redundancy by IL-2, IL-4, IL-7, IL-13, and IL-15. Immunity 1995;2:331–9.
37. Hale MB, Krutzik PO, Samra SS, Crane JM, Nolan GP. Stage dependent aberrant regulation of cytokine-STAT signaling in murine systemic lupus erythematosus. PLoS One 2009;4:e6756.
38. Basu R, Hatton RD, Weaver CT. The Th17 family: flexibility follows function. Immunol Rev 2013;252:89–103.
39. Park MH, D'Agati V, Appel GB, Pirani CL. Tubulointerstitial disease in lupus nephritis: relationship to immune deposits, interstitial inflammation, glomerular changes, renal function, and prognosis. Nephron 1986;44:309–19.
40. Wehrmann M, Bohle A, Held H, Schumm G, Kendziorra H, Pressler H. Long-term prognosis of focal sclerosing glomerulonephritis: an analysis of 250 cases with particular regard to tubulointerstitial changes. Clin Nephrol 1990;33:115–22.
41. Bettelli E, Oukka M, Kuchroo VK. TH-17 cells in the circle of immunity and autoimmunity. Nat Immunol 2007;8:345–50.
42. Wong CK, Ho CY, Li EK, Lam CW. Elevation of proinflammatory cytokine (IL-18, IL-17, IL-12) and Th2 cytokine (IL-4) concentrations in patients with systemic lupus erythematosus. Lupus 2000;9:589–93.
43. Crispin JC, Oukka M, Bayliss G, Cohen RA, Beek CA, Stillman IE, et al. Expanded double negative T cells in patients with systemic lupus erythematosus produce IL-17 and infiltrate the kidneys. J Immunol 2008;181:8761–6.
44. Wang Y, Ito S, Chino Y, Goto D, Matsumoto I, Murata H, et al. Laser microdissection-based analysis of cytokine balance in the kidneys of patients with lupus nephritis. Clin Exp Immunol 2010;159:1–10.
45. Liu J, Karypis G, Hippen KL, Vegoe AL, Ruiz P, Gilkeson GS, et al. Genomic view of systemic autoimmunity in MRLlpr mice. Genes Immun 2006;7:156–68.
46. Schwarting A, Wada T, Kinoshita K, Tesch G, Kelley VR. IFN-γ receptor signaling is essential for the initiation, acceleration, and destruction of autoimmune kidney disease in MRL-Fas^{lpr} mice. J Immunol 998;161:494–503.
47. Yang XP, Ghoreschi K, Steward-Tharp SM, Rodriguez-Canales J, Zhu J, Grainger JR, et al. Opposing regulation of the locus encoding IL-17 through direct, reciprocal actions of STAT3 and STAT5. Nat Immunol 2011;12:247–54.
48. Matsumoto M, Tanaka N, Harada H, Kimura T, Yokochi T, Kitagawa M, et al. Activation of the transcription factor ISGF3 by interferon-γ. Biol Chem 1999;380:699–703.
49. Hall JC, Casciola-Rosen L, Berger AE, Kapsogeorgou EK, Cheadle C, Tzioufas AG, et al. Precise probes of type II interferon activity define the origin of interferon signatures in target tissues in rheumatic diseases. Proc Natl Acad Sci U S A 2012;109:17609–14.
50. De Weerd NA, Vivian JP, Nguyen TK, Mangan NE, Gould JA, Braniff SJ, et al. Structural basis of a unique interferon-β signaling axis mediated via the receptor IFNAR1. Nat Immunol 2013;14:901–7.
51. Baccala R, Gonzalez-Quintial R, Schreiber RD, Lawson BR, Kono DH, Theofilopoulos AN. Anti-IFN-α/β receptor antibody treatment ameliorates disease in lupus-predisposed mice. J Immunol 2012;189:5976–84.
52. Mangini AJ, Lafyatis R, Van Seventer JM. Type I interferons inhibition of inflammatory T helper cell responses in systemic lupus erythematosus. Ann N Y Acad Sci 2007;1108:11–23.